

# Ripening of nanowire-supported gold nanoparticles

Timothy Turba · M. Grant Norton ·  
Ishwar Niraula · David N. McIlroy

Received: 12 August 2008 / Accepted: 13 December 2008  
© Springer Science+Business Media B.V. 2008

**Abstract** Gold nanoparticles have applications ranging from catalysts for low temperature oxidation of CO to solar energy capture in the infrared. For all these applications, particle size and shape are critical. In this study, nanoparticle gold formed on GaN nanowires by plasma-enhanced chemical vapor deposition was annealed at temperatures ranging from 150 to 270 °C for 24 h. Particle size was measured before and after annealing using a field emission scanning electron microscope. Ripening of the gold particles was observed even at the lowest annealing temperatures of the study. The particle growth kinetics showed an Arrhenius relationship with activation energy of 27.38 kJ/mol. This value suggests that ripening occurs by particle migration and coalescence rather than adatom diffusion.

**Keywords** Gold nanoparticles · Ripening · GaN nanowires · Particle migration and coalescence · Nanomaterials · Nanocomposites

## Introduction

Nanomaterials are of great technological interest, for example in clean technology applications, because of their unique properties that differ from their bulk material counterparts (e.g., Sahaym and Norton 2008). Catalysis is often enhanced in nanomaterials, as their high surface-to-volume ratio allows more active sites to be exposed. Gold may be the most important of all the nanomaterials. Although it is the least reactive metal, gold nanoparticles are extremely active and selective in various catalytic reactions when under 5 nm in diameter (Haruta 1997). Nanoparticle gold catalysts can be useful in a variety of reactions ranging from hydrogenation to reduction and decomposition of NO and NO<sub>2</sub> to CO oxidation (e.g., Haruta 1997; Schimpf et al. 2002). Gold is preferred in many reactions over common precious metal catalysts, such as Pt and Pd, because it is more reactive at lower temperatures (Haruta 1997). Most automobile pollution occurs in the first 5 min of driving, as the Pt and Pd in the catalytic converter are unable to oxidize gases like CO under 200 °C (Campbell 2004). Nanoparticle gold could overcome this limitation, as it has been demonstrated to oxidize CO at room temperature (Haruta 1997).

Supported gold nanoparticles tend to lose their catalytic activity if they are larger than about 5 nm in diameter. Since many reactions, even involving nanoparticle gold run at elevated temperatures, it is imperative to understand the thermal stability of the

---

T. Turba (✉) · M. G. Norton  
School of Mechanical and Materials Engineering,  
Washington State University, Pullman,  
WA 99164-2920, USA  
e-mail: tturba@wsu.edu

I. Niraula · D. N. McIlroy  
Department of Physics, University of Idaho,  
Moscow, ID 83844-0903, USA

particles and the extent to which ripening may occur. For example, very small gold nanoparticles have been determined to be cuboctahedral; as the particles grow, the fraction of corner and edge sites decreases when compared to those on the {111} and {100} planes (Schimpf et al. 2002). Consequently, the selectivity of the catalyst for a specific reaction could change over the period of operation.

In addition to their reactivity, gold nanoparticles have been shown to absorb light through surface plasmon resonance (SPR). Plasmon resonance can be tuned to different wavelengths facilitating a wide variety of applications, including color filters, photonic band-gap materials, and all optical switching devices (Eilers et al. 2006). The size and aspect ratio of the gold nanoparticles determines the wavelength of light that is absorbed due to SPR (e.g., Foss et al. 1994; Link et al. 1999). Thus, if the nanoparticle size could be strictly controlled either during deposition or post-deposition processing, it may be possible to create an array of gold nanoparticles that absorb the broad solar spectrum. Utilizing such an array as a solar cell could lead to increases in efficiency over present photovoltaic devices. However, if solar cells were made using gold nanoparticles coupled with some form of light focusing arrangement, what would be the stability of the particles over time at temperature? Commercial cells can reach temperatures up to 90 °C during normal operation (Malik and Damit 2003). In such cases, the thermal stability of the gold nanoparticles may become important because if the nanoparticles ripen at these temperatures, the wavelengths of light adsorbed would change as well.

Supported gold nanoparticles have also been shown to make sensitive gas sensors (e.g., Dobrokhotov et al. 2006a, b). The depletion layer created by the nanoparticle gold on a semiconductor surface allows for detection of reactive gases like methane. Thermally induced changes in particle size could significantly affect the behavior and performance of these types of devices.

Classic sintering theories predict particle growth at about half the melting temperature, which for bulk gold would be 532 °C (the melting temperature of gold is 1064 °C). However, studies have shown that the melting temperature of nanoparticle gold <5 nm in diameter is extremely depressed (Buffat and Borel 1976). At 2 nm, the gold particles melt at temperatures as low as 327 °C. Consequently, it might be

expected that gold nanoparticles ripen at temperatures much lower than those associated with bulk polycrystalline gold.

In this study, temperature-dependent size changes of gold nanoparticles nucleated on gallium nitride nanowires are presented. This system was selected because it has been demonstrated to act as a sensitive gas sensor for species such as methane and CO (Dobrokhotov et al. 2006a, b).

## Experimental details

The GaN nanowires were synthesized on silicon substrates through the reaction of gallium and ammonia (NH<sub>3</sub>) in a standard tubular flow furnace at 950 °C and atmospheric pressure. The process has been described in more detail elsewhere (Dobrokhotov et al. 2006a, b). The nanowires grow via the vapor-liquid-solid (VLS) mechanism and have diameters from 30 to 180 nm.

Gold nanoparticles were deposited onto the GaN nanowires by plasma-enhanced chemical vapor deposition (PECVD) using a parallel plate chamber (LaLonde et al. 2005). The system was operated at 13.56 MHz. Argon was used as the carrier gas and the substrate was heated to 300 °C for the gold deposition. The baseline vacuum pressure for the system was 35 mT, and the pressure with the Ar gas and Au precursor (98% pure dimethyl(acetylacetonate) gold (III), Strem Chemicals, Inc.) was 325 mT prior to deposition. For the parallel plate system, the first plate contained a nozzle to aim the precursor and carrier gas, the second plate was the ground that had a variable transformer controlled heater and the sample held in place. Under these conditions, the typical average gold particle size is 10 nm. This size of particle is straight-forward to image in the scanning electron microscope and permits the determination of size change with annealing. In this study, variations in the deposition parameters and their effect on the initial size of the gold nanoparticles were not determined. However, earlier work by LaLonde et al. (2005) demonstrated that both temperature and pressure can affect the size of the deposited nanoparticles.

The gold-nanoparticle-decorated nanowire samples were annealed in a box furnace in air for a period of 24 h. Annealing temperatures ranged from 150 to

270 °C. Based on the work of Buffat and Borel, this range of annealing temperatures corresponds to 15–33% of the melting temperature of the gold nanoparticles used in this study. The maximum percent of the melting temperature was determined by taking 5 nm to be the smallest gold nanoparticle observed by the SEM, and then taking the ratio of the depressed melting temperature against the highest annealing temperature. Likewise, the minimum percent of the melting temperature was determined by taking the largest particles (no melting point depression), and then taking the ratio of the full melting temperature against the lowest annealing temperature. Before and after annealing, images were taken with a field emission scanning electron microscope (FESEM, FEI Sirion) operated at 10 kV. No sample coating was used, as charging was not an issue. Nanoparticle size was measured by recording the longest observed diameter of each particle. A minimum of 200 nanoparticles was measured on a single nanowire and multiple nanowires were observed for each sample in an attempt to obtain statistically significant and reproducible data.

Other groups have used related approaches to determine size changes in supported nanoparticles. Zhu et al. (2007) and Bore et al. (2004) used transmission electron microscopy (TEM) measurements to determine the ripening of silver nanoparticles on carbon nanotubes and the thermal stability in gold nanoparticles in mesoporous silica, respectively. Mitchell et al. (2001) estimated the size of Au nanoclusters on TiO<sub>2</sub> using scanning tunneling microscope corrugation profiles, and then binning the diameter measurements by increments of 0.1 nm.

## Results and discussion

Figure 1 shows a low-magnification image of a mat of GaN nanowires coated with gold nanoparticles. The size of the gold particles was found to be independent of the nanowire diameter; so, nanowires were typically selected at random for the nanoparticle analysis. The average diameter of the nanowires in Fig. 1 is approximately 100 nm.

Figure 2a and b show before and after images of a gold-coated GaN nanowire annealed at 270 °C, which was the maximum temperature studied. The

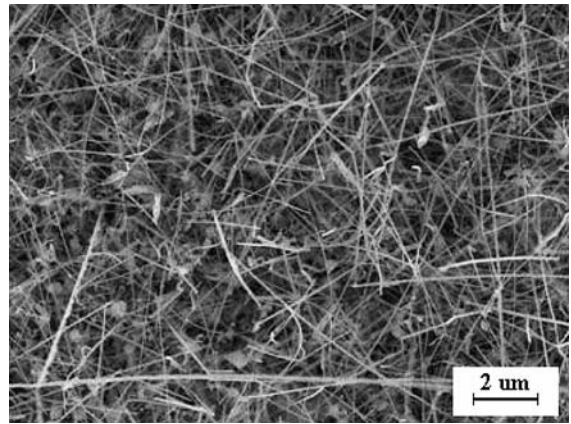


**Fig. 1** Low-magnification SEM image of a mat of GaN nanowires decorated with Au nanoparticles

diameter of the nanowire in both Fig. 2a and b is 130 nm. The gold nanoparticles exhibited growth upon heating as can be seen by comparison of the two images. The diameter of the gold nanoparticles was determined to have increased by 77% upon annealing at 270 °C for 24 h. An increase in particle size was observed for all the annealing temperatures used in this study as shown in Table 1. Standard deviations as well as average size are given.

What was also evident is that annealing caused an increase in the aspect ratio of many of the gold nanoparticles as shown, for example, in Fig. 2c. This observation accounts for the larger standard deviations determined for the annealed nanoparticles and also the particularly large value for the sample annealed at 270 °C. Typical histograms comparing nanoparticle size distributions for the as-grown and annealed particles are given in Fig. 3. Note that in all measurements, it is the largest dimension that is reported.

Nanoparticle size was found to increase exponentially with annealing temperature, as shown by the growth rate  $k$ , which follows an Arrhenius relationship of the form:

$$k = k_0 \exp\left(\frac{-Q}{RT}\right) \quad (1)$$

$ck_0$  is a pre-exponential frequency factor,  $Q$  is the activation energy,  $R$  is the gas constant, and  $T$  is the absolute temperature. Figure 4 shows an Arrhenius plot of the nanoparticle growth rate after annealing. The activation energy was calculated to be 27.38 kJ/mol.

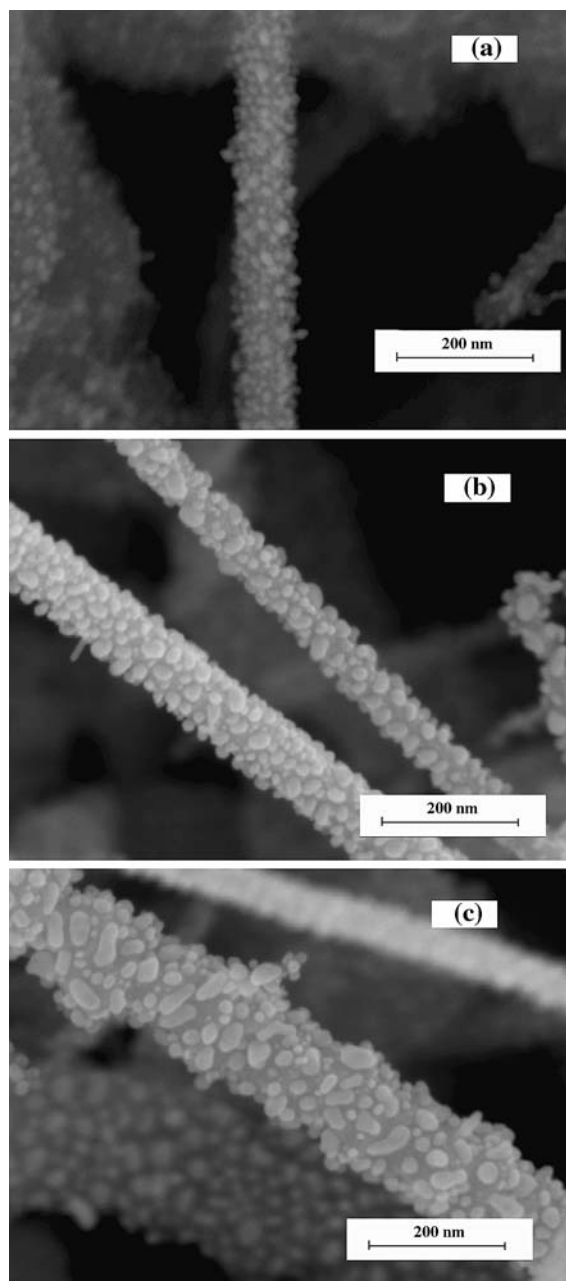


**Fig. 2** SEM images of **a** before and **b, c** after annealing at 270 °C for 24 h. Figure **c** exhibits the increased aspect ratio of the gold nanoparticles

In order to determine the possible growth mechanism for the gold nanoparticles, it is instructive to compare the activation energy determined in this study with the values in the literature. Thermally induced particle growth involves either migration of adatoms (Ostwald ripening) or migration and

**Table 1** Average diameter of gold nanoparticles ( $D_0$ ) and diameter after annealing ( $D_T$ ) for different temperatures ( $T$ )

$T$ [°C]	$D_0$ [nm]	SD	$D_T$ [nm]	SD	Growth rate, $k$ (%)
150	11.73	6.44	12.81	6.81	9.21
171	9.92	2.91	11.78	3.52	18.81
215	10.6	2.87	13.00	4.06	22.64
250	10.03	3.13	13.37	4.42	33.35
270	13.32	3.91	23.59	12.01	77.03

coalescence of nanoparticles (Wynblatt and Gjostein 1975, 1976). In the former case, atomic species from the smaller particles either diffuse along the substrate surface or via the vapor phase due to chemical potential differences between the smaller and larger particles. In the latter case, smaller particles migrate on the substrate surface and coalesce with the larger particles causing an increase in size.

The activation energy for grain growth in bulk polycrystalline gold is 84.9 kJ/mol (Landolt-Boernstein 1990). This value is for grain boundary self-diffusion and reflects the large size of the gold atoms. Similar values have been obtained for electrotransport in gold thin films (Hummel and Geier 1975). The activation energy for grain growth in nano-crystallite gold films has been experimentally determined to be 29.5 kJ/mol (Yevtushenko et al. 2006). This value is much lower than that for bulk gold, which has been attributed to the difference in the grain boundary structure between the nanostructured and coarse-grained materials.

Activation energies for adatom surface diffusion of gold range from about 7 to 16 kJ/mol based on the supporting substrate (LaLonde et al. 2005; Venables 1994; Parker et al. 1999). The activation energy obtained in this study for the ripening of gold nanoparticles is significantly higher than in these cited studies for adatom diffusion. The implication is that growth occurs by particle migration and coalescence rather than atom diffusion. As recognized by other groups, it is difficult to obtain a detailed mechanistic insight based solely on the change in particle size distribution before and after heating (Datye et al. 2006). However, the present results would indicate that the more likely growth mechanism is the migration of gold particles and their subsequent coalescence. This mechanism is the one that has been proposed for the ripening of silver nanoparticles on carbon nanotubes (Zhu et al. 2007) and

**Fig. 3** Before (*top image*) and after (*bottom image*) histograms of the sample annealed at 250 °C for 24 h

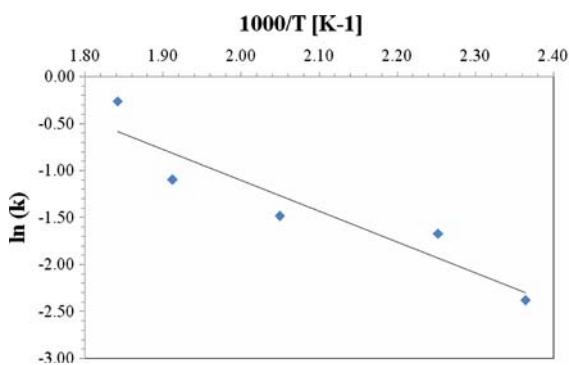
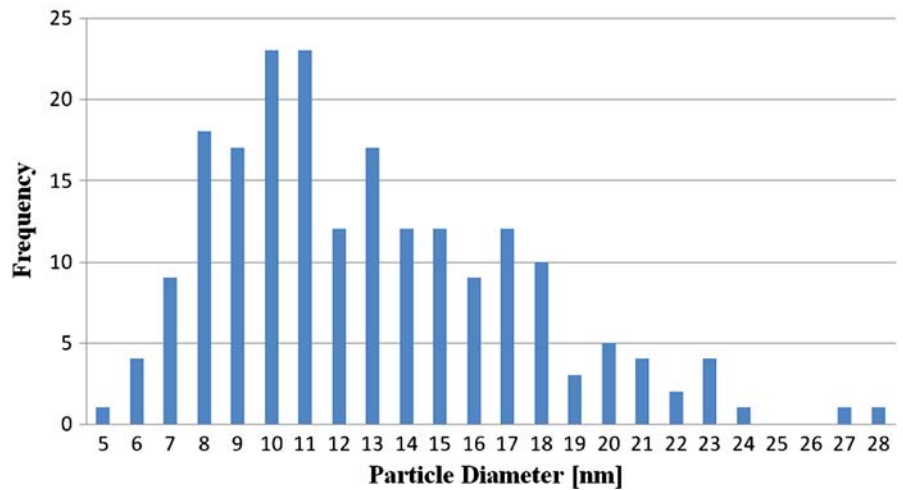
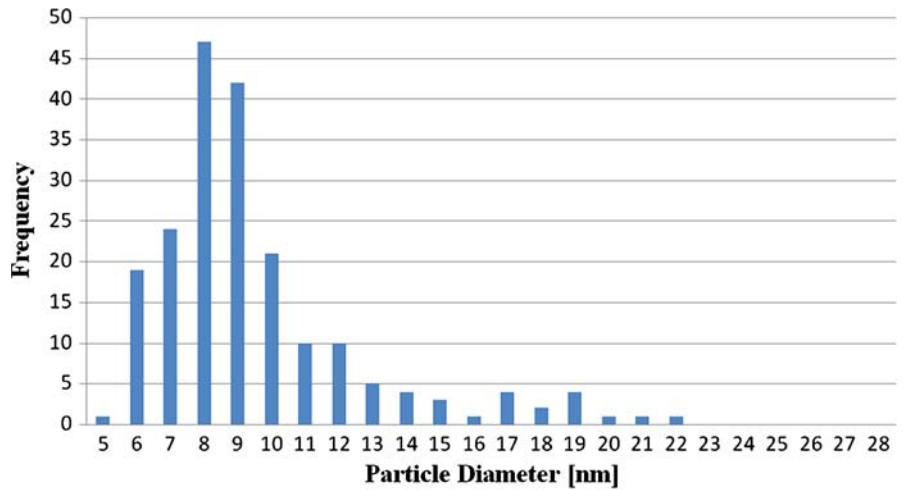


**Fig. 4** Arrhenius plot of nanoparticle growth rate against inverse of the annealing temperature

for small palladium clusters on single crystal TiO<sub>2</sub> (Jak et al. 2000). The close agreement between the activation energy obtained in our study and that reported for grain

growth in nano-crystalite gold thin films suggest that particle coalescence (i.e., sintering) may be the overall rate-limiting step in the ripening process.

Using a similar argument of Zhu et al. (2007), our results show that the interaction between the gold nanoparticles and the GaN nanowires is relatively weak and of the van der Waals type. However, we do know that there are electronic interactions between gold nanoparticles and GaN nanowires and that this interaction can be modified by physisorption of different species in the vapor phase (Dobrokhotov et al. 2006a, b). Gold atoms have the highest electron affinity of any metal and thus electron transfer into the gold nanoparticles is likely. Thus, an interesting experiment suggests itself and that is to conduct annealing in various atmospheres and determine its effect on ripening kinetics.

The observed increase in the aspect ratio of the gold nanoparticles upon annealing, as illustrated in Fig. 2c, is of interest and tends to support the migration/coalescence mechanism for ripening. A practical outcome of the deviation from an equiaxed shape is its effect on SPR absorption. Metal nanoparticles deviating from a spherical or equiaxed shape exhibit multiple polarization dipoles corresponding to secondary SPR wavelengths (Link et al. 1999). A single axis extension of a spherical particle into a non-equiaxed particle results in transverse (about the circular cross section) and longitudinal (about the long axis) resonance modes (Link et al. 1999; Shalaev 2002).

## Conclusion

Gold nanoparticles were deposited onto GaN nanowires by PECVD and annealed for 24 h in air at temperatures ranging from 150 to 270 °C. The annealed nanoparticles exhibited an exponential increase in size with increasing temperature, with activation energy of 27.38 kJ/mol. This value suggests that ripening occurs by particle migration and coalescence rather than via Ostwald ripening. The increase in the aspect ratio of the gold nanoparticles following annealing supports the proposed growth mechanism.

**Acknowledgment** DNM would like to acknowledge the support from the University of Idaho's Biological Applications of Nanotechnology (BANTech) Presidential Initiative and the National Science Foundation (EPS0132626).

## References

- Bore MT, Pham HN, Ward TL and Datye AK (2004) Role of pore curvature on the thermal stability of gold nanoparticles in mesoporous silica. *Chem Commun (Camb)* 2620–2621. doi:[10.1039/b407575g](https://doi.org/10.1039/b407575g)
- Buffat P, Borel J-P (1976) Size effect on the melting temperature of gold particles. *Phys Rev A* 13:2287–2298. doi:[10.1103/PhysRevA.13.2287](https://doi.org/10.1103/PhysRevA.13.2287)
- Campbell CT (2004) The active site in nanoparticle gold catalysis. *Science* 306:234–235. doi:[10.1126/science.11042467](https://doi.org/10.1126/science.11042467)
- Datye AK, Xu Q, Kharas KC, McCarty JM (2006) Particle size distributions in heterogeneous catalysts: what do they tell us about the sintering mechanism? *Catal Today* 111:59–67. doi:[10.1016/j.cattod.2005.10.013](https://doi.org/10.1016/j.cattod.2005.10.013)
- Dobrokhotov V, McIlroy DN, Norton MG, Abuzir A, Yeh WJ, Stevenson I, Pouy R, Bochenek J, Cartwright M, Wang L, Dawson J, Beaux M, Berven CA (2006a) Principles and mechanisms of gas sensing by GaN nanowires functionalized with gold nanoparticles. *J Appl Phys* 99:104302–104307. doi:[10.1063/1.2195420](https://doi.org/10.1063/1.2195420)
- Dobrokhotov V, McIlroy DN, Norton MG, Berven CA (2006b) Transport properties of hybrid nanoparticle–nanowire systems and their application to gas sensing. *Nanotechnology* 17:4135–4142. doi:[10.1088/0957-4484/17/16/024](https://doi.org/10.1088/0957-4484/17/16/024)
- Eilers H, Biswas A, Pounds TD, Norton MG, Elbahri M (2006) Teflon AF/Ag nanocomposites with tailored optical properties. *J Mater Res* 21:2168–2171. doi:[10.1557/JMR.2006.0267](https://doi.org/10.1557/JMR.2006.0267)
- Foss CA Jr, Hornyak GL, Stockert JA, Martin CR (1994) Template-synthesized nanoscopic gold particles: optical spectra and the effects of particle size and shape. *J Phys Chem* 98:2963–2971. doi:[10.1021/j100062a037](https://doi.org/10.1021/j100062a037)
- Haruta M (1997) Size- and support-dependency in the catalysis of gold. *Catal Today* 36:153–156. doi:[doi:10.1016/S0920-5861\(96\)00208-8](https://doi.org/10.1016/S0920-5861(96)00208-8)
- Hummel RE, Geier HJ (1975) Activation energy for electrotransport in thin silver and gold films. *Thin Solid Films* 25:335–342. doi:[10.1016/0040-6090\(75\)90053-X](https://doi.org/10.1016/0040-6090(75)90053-X)
- Jak MJJ, Konstapel C, van Kreuningen A, Verhoeven J, Frenken JWM (2000) Scanning tunneling microscopy study of the growth of small palladium particles on TiO<sub>2</sub>(110). *Surf Sci* 457:295–310. doi:[10.1016/S0039-6028\(00\)00431-3](https://doi.org/10.1016/S0039-6028(00)00431-3)
- LaLonde AD, Norton MG, Zhang D, Gangadean D, Alkhateeb A, Padmanabhan R, McIlroy DN (2005) Controlled growth of gold nanoparticles on silica nanowires. *J Mater Res* 20:3021–3027. doi:[10.1557/JMR.2005.0368](https://doi.org/10.1557/JMR.2005.0368)
- Landolt-Boernstein (1990) Numerical data and functional relationships in science and technology, diffusion in solid metals and alloys, vol 26. Springer, Berlin, p 640
- Link S, Mohamed MB, El-Sayed MA (1999) Simulation of the optical absorption spectra of gold nanorods as a function of their aspect ratio and the effect of the medium dielectric constant. *J Phys Chem B* 103:3073–3077. doi:[10.1021/jp990183f](https://doi.org/10.1021/jp990183f)
- Malik AQ, Damit S (2003) Outdoor testing of single crystal silicon solar cells. *Renew Energy* 28:1433–1445. doi:[10.1016/S0960-1481\(02\)00255-0](https://doi.org/10.1016/S0960-1481(02)00255-0)
- Mitchell CEJ, Howard A, Carney M, Egdell RG (2001) Direct observation of behaviour of Au nanoclusters on TiO<sub>2</sub>(110) at elevated temperatures. *Surf Sci* 490:196–210. doi:[10.1016/S0039-6028\(01\)01333-4](https://doi.org/10.1016/S0039-6028(01)01333-4)
- Parker SC, Grant AW, Bondzie VA, Campbell CT (1999) Island growth kinetics during the vapor deposition of gold onto TiO<sub>2</sub>(110). *Surf Sci* 441:10–20. doi:[10.1016/S0039-6028\(99\)00753-0](https://doi.org/10.1016/S0039-6028(99)00753-0)
- Sahaym U, Norton MG (2008) Advances in the application of nanotechnology in enabling a 'hydrogen economy'. *J Mater Sci* 43:5395–5429. doi:[10.1007/s10853-008-2749-0](https://doi.org/10.1007/s10853-008-2749-0)
- Schimpf S, Lucas M, Mohr C, Roddemerck U, Brückner A, Radnik J, Hofmeister H, Claus P (2002) Supported gold nanoparticles: in-depth catalyst characterization and application in hydrogen and oxidation reactions. *Catal Today* 72:63–78. doi:[doi:10.1016/S0920-5861\(01\)00479-5](https://doi.org/10.1016/S0920-5861(01)00479-5)
- Shalaev VM (2002) Optical nonlinearities of fractal composites. *Top Appl Phys* 82:93–114. doi:[10.1007/3-540-44948-5\\_5](https://doi.org/10.1007/3-540-44948-5_5)
- Venables JA (1994) Atomic processes in crystal growth. *Surf Sci* 299–300:798–817. doi:[10.1016/0039-6028\(94\)90698-X](https://doi.org/10.1016/0039-6028(94)90698-X)

Wynblatt P, Gjostein NA (1975) Supported metal crystallites. *Prog Solid State Chem* 9:21–58. doi:[10.1016/0079-6786\(75\)90013-8](https://doi.org/10.1016/0079-6786(75)90013-8)

Wynblatt P, Gjostein NA (1976) Particle growth in model supported metal catalysts—I Theory. *Acta Metall* 24: 1165–1174. doi:[10.1016/0001-6160\(76\)90034-1](https://doi.org/10.1016/0001-6160(76)90034-1)

Yevtushenko O, Natter H, Hempelmann R (2006) Grain-growth kinetics of nanostructured gold. *Thin Solid Films* 515:353–356. doi:[10.1016/j.tsf.2005.12.098](https://doi.org/10.1016/j.tsf.2005.12.098)

Zhu L, Lu G, Mao S, Chen J (2007) Ripening of silver nanoparticles on carbon nanotubes. *J Nanopart Res* 2:149–156. doi:[doi:10.1142/S1793292007000507](https://doi.org/10.1142/S1793292007000507)